Available online at www.sciencedirect.com

ScienceDirect

journal homepage: www.intl.elsevierhealth.com/journals/dema

Fatigue failure load and finite element analysis of multilayer ceramic restorations

K.C. Archangelo[a], L.F. Guilardi[b], D. Campanelli[c], L.F. Valandro[d], A.L.S. Borges[e,*]

[a] Institute of Science and Technology of São Jose dos Campos, São Paulo State University (UNESP), Sao Jose dos Campos, Brazil
[b] Post-Graduation Program in Oral Science, Santa Maria Federal University (UFSM), Santa Maria, Brazil
[c] Institute of Science and Technology of São Jose dos Campos, São Paulo State University (UNESP), Sao Jose dos Campos, Brazil
[d] Faculty of Odontology, Santa Maria Federal University (UFSM), Santa Maria, Brazil
[e] Institute of Science and Technology of São Jose dos Campos, São Paulo State University (UNESP), Sao Jose dos Campos, Brazil

ARTICLE INFO

Article history:
Received 9 March 2018
Received in revised form
12 July 2018
Accepted 11 October 2018

Keywords:
Ceramics
Dental materials
Elastic modulus
Tensile strength
Fatigue
Finite element analysis

ABSTRACT

Objective. To evaluate the fatigue failure load via staircase approach and stress distribution via FEA of different ceramic configurations arranged in multilayers composed of ceramic materials with different elastic moduli and compare them to monolayer models.

Methods. CAD–CAM ceramic blocks were used to shape 0.3 mm and 1.5 mm thick discs, corresponding to: feldspathic (F), 64 GPa; lithium disilicate (L), 95 GPa; and Yttrium-partially stabilized tetragonal zirconia (Y-TZP) (Y), 209.3 GPa. The 0.3 mm discs were arranged in 4 layers cemented with resin cement (Multilink N), and the 1.5 mm discs were not treated, in such a way that the final thickness of all specimens was 1.5 mm (±0.15 mm). The following 6 groups were tested: F (F: monolithic); L (L: monolithic); LLFF (L + L + F + F); FFLL (F + F + L + L); YLFF (Y + L + F + F); YLLF (Y + L + L + F). The loads-to-fracture were obtained using the biaxial flexural strength test until failure and the data were run using one-way ANOVA and Tukey's multiple comparisons ($\alpha = 0.05$) tests. The biaxial bending test was also simulated through finite element analysis (FEA) to identify the tensile stress generated at each layer of the groups. Mean fatigue failure load (100,000 cycles; 20 Hz) was determined using the staircase approach. The fracture analysis was performed by stereomicroscope and scanning electron microscopy.

Results. The load to fracture (N) were obtained as follows: L (592.9 ± 73.8)^{D} > FFLL (319.78 ± 43.59)^{C} > YLLF (246.75 ± 24.89)^{B} > F (167.13 ± 9.84)^{A} > YLFF (166.51 ± 15.24)^{A} > LLFF (165.46 ± 22.75)^{A}; and the fatigue failure load (N): L (310.92 ± 26.73)^{F} > FFLL (190.17 ± 8.32)^{E} > F (106.21 ± 2.81)^{D} > YLLF (96.48 ± 5.73)^{C} > YLFF (89.56 ± 2.38)^{B} > LLFF (77.23 ± 6.33)^{A}. The origin of all of the tested specimens was located at the tensile region of the discs, as encountered in FEA.

* *Corresponding author at*: Institute of Science and Technology of São Jose dos Campos, São Paulo State University (UNESP), Engenheiro Francisco José Longo Avenue, 777 Jardim São Dimas, São José dos Campos, São Paulo, Brazil.
E-mail addresses: karenarchangelo@yahoo.com.br (K.C. Archangelo), luisfguilardi@hotmail.com (L.F. Guilardi), dayanacampanelli@gmail.com (D. Campanelli), lfvalandro@hotmail.com (L.F. Valandro), alexandre.borges@unesp.br, aleborges@ict.unesp.br (A.L.S. Borges).
https://doi.org/10.1016/j.dental.2018.10.006

Significance. The material under tensile stress is determinant for the restoration's strength and the adhesive interface negatively influenced the mechanical behavior of the multilayer structures.

1. Introduction

Ceramic materials have been widely used in restorative treatments due to excellent qualities as such superior aesthetics, biocompatibility, chemical stability, wear resistance, low biofilm adhesion and color stability [1]. In addition, the constant optimization of its microstructure and physical properties has allowed its use in areas of great masticatory effort such as posterior regions [2]. Regardless of the type of ceramic material used, clinical researches point to an estimated survival rate of around 90% after 5 years [3–7]. The main failure mode reported for bilayered ceramics is the chipping of the veneering ceramic due to the thermal expansion mismatch between core and veneer, and/or due to the lack of support for the veneering ceramic as a result of an incorrect framework design [7,8].

The fracture behavior of all ceramic restorations is related to their mechanical properties. Dental ceramics tend to fail at the critical strain of 0.1%. In this sense, any increase in strength and toughness can be achieved by an increase in the elastic modulus (*E*) [9]. However, ceramics are incapable of reversible deformation since the material presents low tensile strength, consequently tending to catastrophic failure [10].

Bioinspired multilayer configurations have been proposed [11–14] in order to improve the fracture strength of ceramic materials. The human tooth is a graded structure composed by a mineralized matrix and organic reinforcements, consisting of three basic structural parts: enamel, dentin and the dentin–enamel junction [15], presenting a decreased *E* from the external surface of the enamel to the internal region of the tooth [16]. This configuration favors the ability of the enamel in resisting to fracture, and crack propagation toward the dentin–enamel junction is always arrested and unable to penetrate the dentin [17].

In traditional ceramic restorations arranged in layers, the ceramic modulus of elasticity in the upper region ranges from 65 to 300 GPa, while in the natural tooth support structure characterized by dentin, the value is approximately 20 GPa [18,19]. The modulus of elasticity of adhesive cements ranges from 2 to 13 GPa [11]. This large difference of modulus of elasticity results in a high stress level that may cause radial cracks in the ceramic veneer [20]. However, this situation does not occur in the natural tooth, which presents a functionally graded layer at the interface between enamel and dentin (dentin–enamel junction) with thickness ranging from 10 to 100 μm [21].

Thus, the aims of this study were to investigate the interaction and the stress distribution between the ceramic materials arranged in layers, and to understand the mechanical behavior, the failure mode and the fracture origin in both monolithic and bioinspired (in layers) ceramic configurations.

2. Materials and methods

The materials used in this study are presented in Table 1.

2.1. Preparation of ceramic discs

Ceramic blocks were rounded to 15 mm diameter (Vita In-Ceram YZ-Y) and 13 mm diameter (IPS e.max CAD-L, Vitablocs Mark II-F) cylinders using a diamond-impregnated drill mounted on a cutting machine. The cylinders were sliced in a saw cutting machine (IsoMet Low Speed, Buehler, IL, USA) at 250 rpm under water-cooling to obtain the discs. Y discs were wet-ground flat with silicon carbide (SiC) (#1200) and sintered according to the manufacturer's instructions (Vita Zyrcomat, Vita Zahnfabrik) following the schedule: temperature elevation time, 1 h; final temperature, 1530 °C; waiting time, 2 h; and cooling temperature, 400 °C. The Y discs were air-abraded with aluminum oxide (50 μm) for 10 s at 2.5 bar pressure and 10 mm distance from the disc to the tip of the micro-etcher (Basic Classic, Renfert, Brazil), and the annealing was set in accordance with the manufacturer's instructions (Atlantis 50P-Platinum, Kota equipments, Brazil): initial temperature, 500 °C; heating rate, 100 °C/min; final temperature, 1000 °C; waiting time, 15 min. The final dimensions were 12 mm in diameter and 0.3 ± 0.03 mm thick measured using a digital micrometer (Mitutoyo Corporation, Tokyo, Japan).

L and F discs were wet-ground flat in a polisher machine (Ecomet 250, Buehler, Lake Bluff, IL, USA) with sequential SiC papers (#400, #800 and #1200). L discs were sintered according to the manufacturer's instructions (Programat P500, Ivoclar Vivadent) following schedule: stand-by temperature, 403 °C; heating rate, 90 °C/min; firing temperature (T1), 820 °C; holding time, 10 min; heating rate, 30 °C/min; firing temperature (T2), 840 °C; holding time, 7 min; long-term cooling, 700 °C. The final dimensions were 12 mm in diameter (ISO 6872) and thickness of 0.3 ± 0.03 mm and 1.5 ± 0.10 mm, measured using a digital micrometer.

All the discs were ultrasonically bathed in 99.8% isopropanol for 380 s and stored dry at room temperature.

2.2. Preparation of specimens

The surfaces that would be in contact with the cement were etched with 10% hydrofluoric acid for 20 s (L) and 60 s (F), then water cleaned.

Cementation of the multilayer group was performed with the aid of a micrometer, which contained two flat metallic plateaus that served as supports for the ceramic discs. The first two discs were positioned between the plateaus that were juxtaposed and the micrometer was reset until the distance mark of zero. The micrometer was opened and the discs were

Table 1 – Commercial name, initials, lot and material properties (elastic modulus — E; and Poisson's ratio — ν) [22–25].

Commercial name	Initials	Lot	E (GPa)	Poisson's ratio (ν)
Vita In-Ceram YZ (40/19, VITA Zahnfabrik, Bad Säckingen, Germany)	Y	48000	209.3	0.32
IPS e.max CAD (HT B1/B40, Ivoclar Vivadent, Schaan, Liechtenstein)	L	U33870	102.7	0.21
Vitablocs Mark II (2 M2C I-40/19, VITA Zahnfabrik)	F	35020	64	0.25
Multilink N (Ivoclar Vivadent)	–	U26911	18.6	0.28
Hydrofluoric acid (Dentsply, Rio de Janeiro, Brazil)	–	124311H	–	–
Monobond N (Ivoclar Vivadent)	–	U29879	–	–
Multilink N Primer A (Ivoclar Vivadent)	–	U12051 U33826	–	–
Multilink N Primer B (Ivoclar Vivadent)	–	U09377 U26409	–	–

Table 2 – Means of load-to-fracture (n = 3), initial load for fatigue test (60% of the monotonic load-to-fracture) and the step size (5% of the initial load) for fatigue tests (Staircase method). Fatigue failure load, standard deviation (SD) and 95% confidence interval (CI) from the Staircase test, and the percentage of decrease comparing the monotonic and fatigue findings.

Groups	Load-to-fracture (N)	Initial load for fatigue test(N)	Step size (N)	Fatigue failure load (N)		Decrease from monotonic to fatigue tests (%)
				Mean (SD)	95% CI[a]	
L	650.65	390.39	19.52	310.92 (26.73)^{F}	291.71–330.12	52.21
FFLL	329.91	197.95	9.90	190.17 (8.32)^{E}	183.88–196.46	42.35
LLFF	147.10	88.26	4.41	77.23 (6.33)^{A}	72.68–81.78	47.50
F	177.01	106.21	5.31	106.21 (2.81)^{D}	103.96–108.46	40.00
YLLF	235.31	141.19	7.06	96.48 (5.73)^{C}	91.29–101.66	59.00
YLFF	149.81	89.88	4.49	89.56 (2.38)^{B}	87.91–91.21	40.21

[a] Different letters indicate statistically significant differences by the overlap of confidence intervals according to Collins [26].

removed. A layer of Monobond N was applied with a microbrush on the pre-treated surfaces of the discs and was allowed to react for 60 s, being dispersed with a strong stream of air. The Multilink N primers A and B were mixed in a 1:1 ratio and applied onto the top surface of the inferior disc with a microbrush and scrubbed for 30 s. Then multilink N cement was applied on the center region of the bottom surface of the superior disc. The two discs were centered between the plateaus of the micrometer that was closed until the pointed distance of 100 μm and allowed to self-cure for 8 min. The subsequent layers were cemented following the same protocol until the specimens were composed of 4 ceramic layers.

Two monolayer groups (F (F), L (L)) and four multilayer groups (FFLL (F + F + L + L); LLFF (L + L + F + F); YLFF (Y + L + F + F) — bioinspired; YLLF (Y + L + L + F) — bioinspired) were composed. The final dimensions were according to ISO 6872 standard, being 12 mm in diameter and 1.5 ± 0.1 mm thick.

2.3. *Biaxial flexural strength (BFS)*

A piston-on-three-ball assembly (ISO 6872:2008) was used to determine the load-to-fracture using a universal testing machine (Emic, DL1000 with a 1 KN load cell, EMIC Test Equipment and Systems Ltd, São José dos Pinhais, Brazil). The ceramic specimen (n = 10 per group) was positioned over the three steel spheres (2.5 mm in diameter, 10 mm equidistant) with a load applied at a rate of 1 mm/min, perpendicular to the center of the top surface of the specimen by a 1.4 mm flat tip of a cylindrical steel piston. The load-to-fracture was reported by tester and data were analyzed by one-way ANOVA and a post hoc Tukey's multi-comparison test ($\alpha = 0.05$).

2.4. *Biaxial flexural fatigue test (Staircase method)*

The fatigue test was performed in an electric machine (Instron ElectroPuls E3000, Instron Corporation, Norwood, USA) following the flexural strength test set up according to ISO 6872, and using the Staircase method described by Collins [26]. The flexural fatigue strength was determined by 100,000 cycles for each specimen; the cyclic load was applied in a sinusoidal approach with a frequency of 20 Hz and the amplitude ranged from a minimum of 10 N (to maintain the piston in intimate contact with the specimen) up to the maximum load attributed for each specimen. To determine the initial load for the first specimen for the fatigue test (estimated fatigue failure load: 60% of the mean load-to-fracture), three specimens of each group were monotonically tested to obtain the mean load-to-fracture value, which is considered as the maximum load supported by the material until its failure. The subsequent specimen was tested with a loading level of approximately 5% (step size) higher or lower than the initial loading level, according to survival or failure (fracture/crack) of the previous specimen, respectively (Table 2). This procedure was repeated until 15 specimens of each group were tested, counting from the first event inversion (survival to failure or vice versa). The mean biaxial flexural fatigue load (FFL), standard deviation (SD) and confidence interval (CI - 95%, 0.05) were calculated based on the least frequent event data (survival or failure) according to the Dixon and Mood method, which involves maximum-likelihood estimation, assuming

that these data follow a normal distribution [26], and using Eqs. (1) and (2):

$$FFL = FFL_0 + d\left[\sum in_i / \sum n_i \pm 1/2\right] \quad (1)$$

$$I = 1.62d\left\{\left[\left(\Sigma n_i \Sigma i^2 n_i - (\Sigma i n_i)^2\right)/(\Sigma n_i)^2\right] + 0.029\right\}$$
$$\text{if}: \left[\left(\Sigma n_i \Sigma i^2 n_i - (\Sigma i n_i)^2\right)/(\Sigma n_i)^2\right] \geq 0.3 \quad (2)$$

where FFL_0 is the lowest flexural fatigue load considered in the analysis, and d is the step size. In Eq. (2), the negative sign was used when the less frequent event was failure and the positive sign was used when the less frequent event was survival. $i = 0$ was the lowest flexural fatigue load level, $i = 1$ the next flexural fatigue load level, and consecutively. n_i is the number of failures or survivals at the given flexural fatigue load level.

The test was scheduled to stop when the specimen failed, and the load until fracture and the number of fragments was registered.

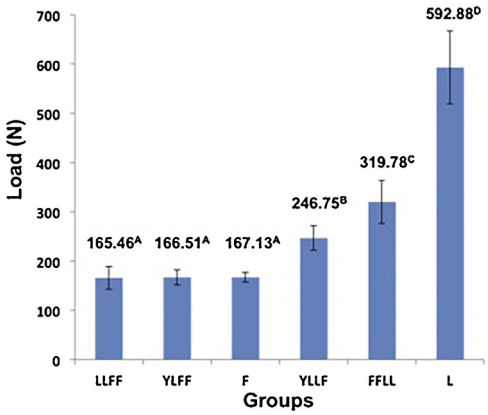

Fig. 1 – Mean values and standard deviation of load-to-fracture (N) in the biaxial flexural strength test. Different capital letters mean statistically significant difference according to ANOVA and a post hoc Tukey's multi-comparison test ($\alpha = 0.05$).

2.5. *Fracture analysis*

After the mechanical tests, the fractured fragments were counted and correlated to its applied load using the Pearson's correlation. The specimens were analyzed in a light microscope (Stereo Discovery V20; Carl Zeiss, Gottingen, Germany) in order to identify the origin of fracture and crack extension in the ceramic layers. The specimens that were not completely separated during the test were sectioned perpendicularly to the fracture mark using a diamond impregnated saw under water-cooling (IsoMet low speed, Buehler). The representative discs from each evaluated condition were submitted to scanning electron microscopy (SEM, Inspect S50, Fei, Oregon, USA). Fractographic landmarks including hackles and Wallner's lines were utilized to track the propagating crack to an initiating origin in the ceramic layers (Figs. 4 and 5).

2.6. *Finite element analysis*

The biaxial flexural strength test was simulated using Finite Element Analysis (FEA). The six experimental groups were initially modeled in CAD (Computer Aided Design) Rhinoceros 5.0 Software (McNeel North America, Seattle, WA, USA) and exported in STEP format to the CAE (Computer Aided Engineering; Software Ansys v. 16.0, Houston, TX, USA) to obtain three-dimensional finite element models. The materials were considered as isotropic, linear and homogeneous, the interfaces between layers were considered ideal with perfect union,

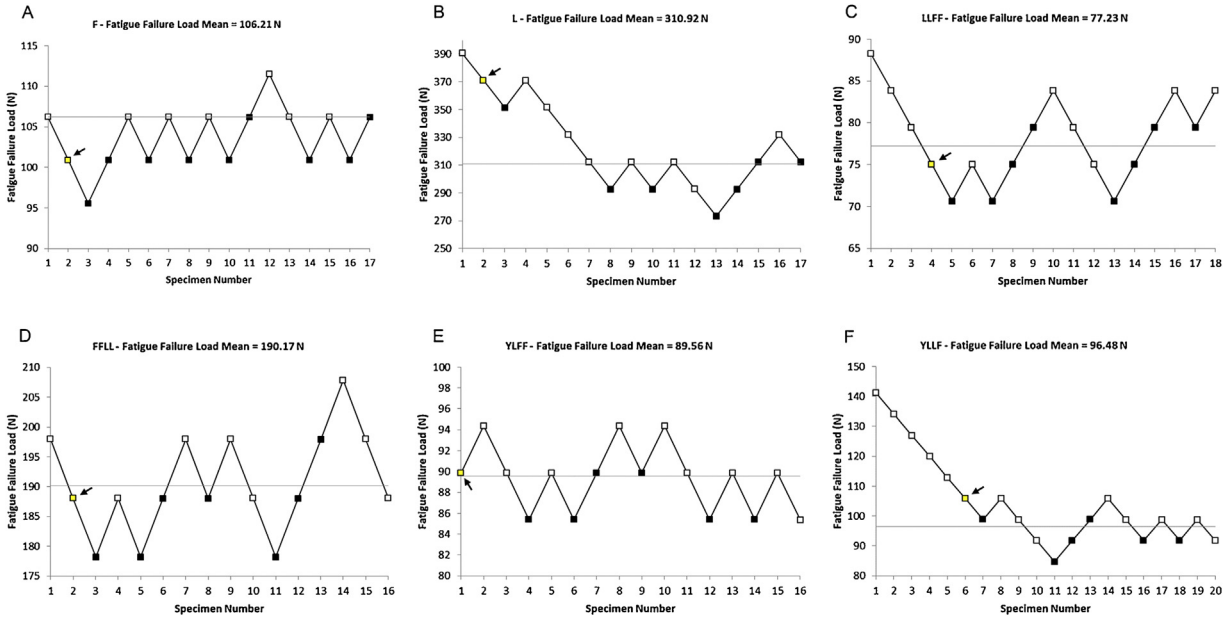

Fig. 2 – Runout (survival) and failure patterns for each group observed during fatigue testing. The yellow box indicated by the arrow represents the load level at which the up-and-down character (Staircase test) started. (For interpretation of the references to colour in this figure legend, the reader is referred to the web version of this article.)

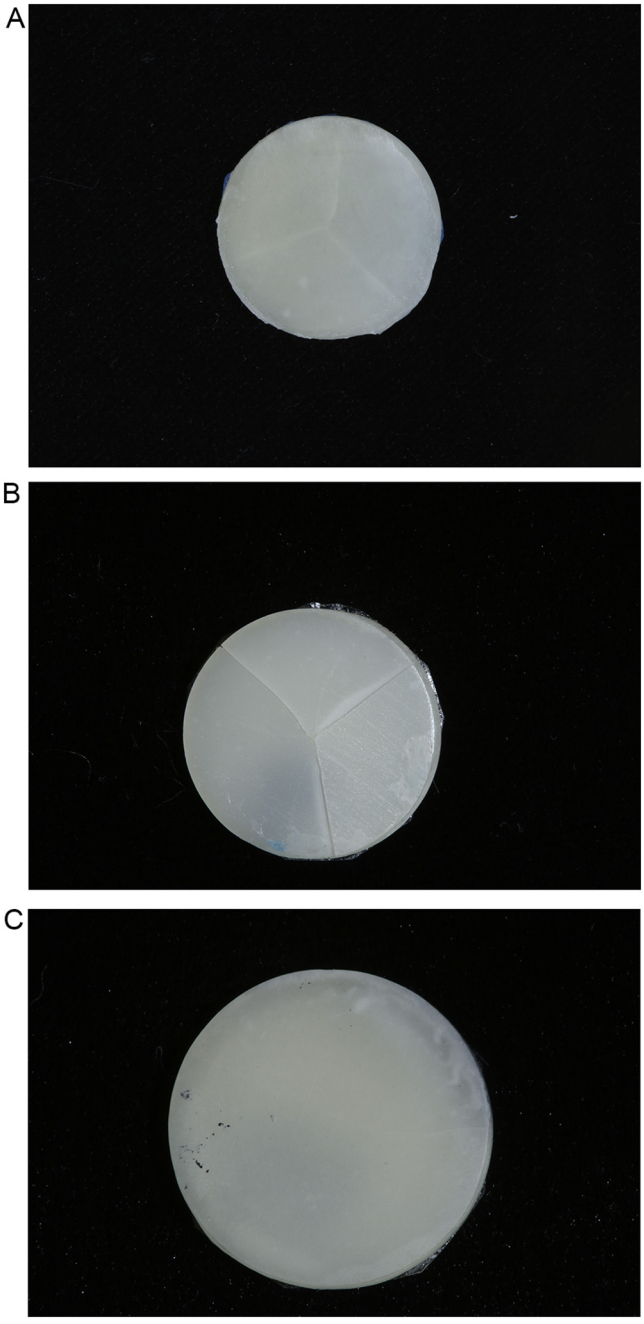

Fig. 3 – Representative images of radial fracture patterns of the specimens. (A) After monotonic test; (B) after fatigue test (groups F, L, LLFF, FFLL); (C) after fatigue test (groups YLFF, YLLF).

and the mesh was a quadratic tetrahedral element. Table 1 presents the elastic modulus (E) and Poisson's ratio for the materials used in this study according to previous studies [22–25]. Six different groups were assumed according to ceramic arrangement as in the previous groups' arrangements described above. The applied load of each group was the mean load to fracture obtained at the biaxial flexural strength test (Table 2). Maximum principal stress (MPS) was calculated for the applied load, normal to the surface, and the fixation was at the base of the preparation. The MPS values of each ceramic layer was calculated in the tensile region and quantitatively compared within the group and among all groups.

3. Results

The ceramic multilayer arrangements resulted in lower mean of load-to-fracture in comparison to the lithium disilicate monolayer group ($p < 0.05$) (Fig. 1). The bioinspired configuration YLLF presented a higher value (246.75 N^B) compared to the monolithic feldspathic material (167.13 N^A), but the monolithic lithium disilicate group (L) presented better performance (592.88 N^D).

The fatigue failure load (N) was significantly higher for L group (310.92 ± 26.73^F) and decreased as follows: FFLL > F > YLLF > YLFF > LLFF. The bioinspired configurations had a decrease in the fatigue failure load compared to load-to-fracture test in 59% for YLLF and 40.21% for YLFF (Table 2), and the monolithic groups had a decrease of 52.21% for L and 40% for F group. The runout (survival) and failure patterns are shown in Fig. 2. Low strength specimens were associated with the presence of two layers of feldspathic ceramic in the tensile region.

Pearson correlation coefficient demonstrated a positive moderate correlation between the number of fracture fragments and load-to-fracture ($r^2 = 0.55$) in the monotonic biaxial flexural strength test, and a positive moderate correlation between the number of fracture fragments and fatigue failure load test ($r^2 = 0.57$). For all specimens subjected to the monotonic and fatigue tests, the monolithic groups failed catastrophically and most specimens of the FFLL group also failed catastrophically, while non-catastrophic failures were predominant in the LLFF, YLFF and YLLF groups.

Fractographic analysis of the tested samples demonstrates radial crack/fracture (Fig. 3) that originates from the bottom surface of the specimens (Figs. 4 and 5). The fracture direction was modified between the layers for the multilayer groups, and it is possible to observe deflection in the crack direction (Figs. 4C–F; 5C–F).

The FEA models (Fig. 6) revealed that the tensile stress region is located in the area compatible with the fracture origin of the specimens for all groups, as shown in the fractographic analysis. The load applied in each group was the load-to-fracture obtained in the monotonic test, so the FEA predicts the MPS generated during the same condition of the BFS test. As observed, the MPS generated in each layer was significantly lower than the flexural strength of the corresponding ceramic material [27].

4. Discussion

The present study considered ceramic materials disposed in layers according to different arrangements, including bioinspired configuration, in order to mimic the mechanical behavior encountered in the natural tooth, which presents a graduated elastic modulus from the outer surface to the inner surface. This configuration offers an alternative to reduce the stress generated in the restoration because of the difference between the elastic moduli of the ceramic layers [20].

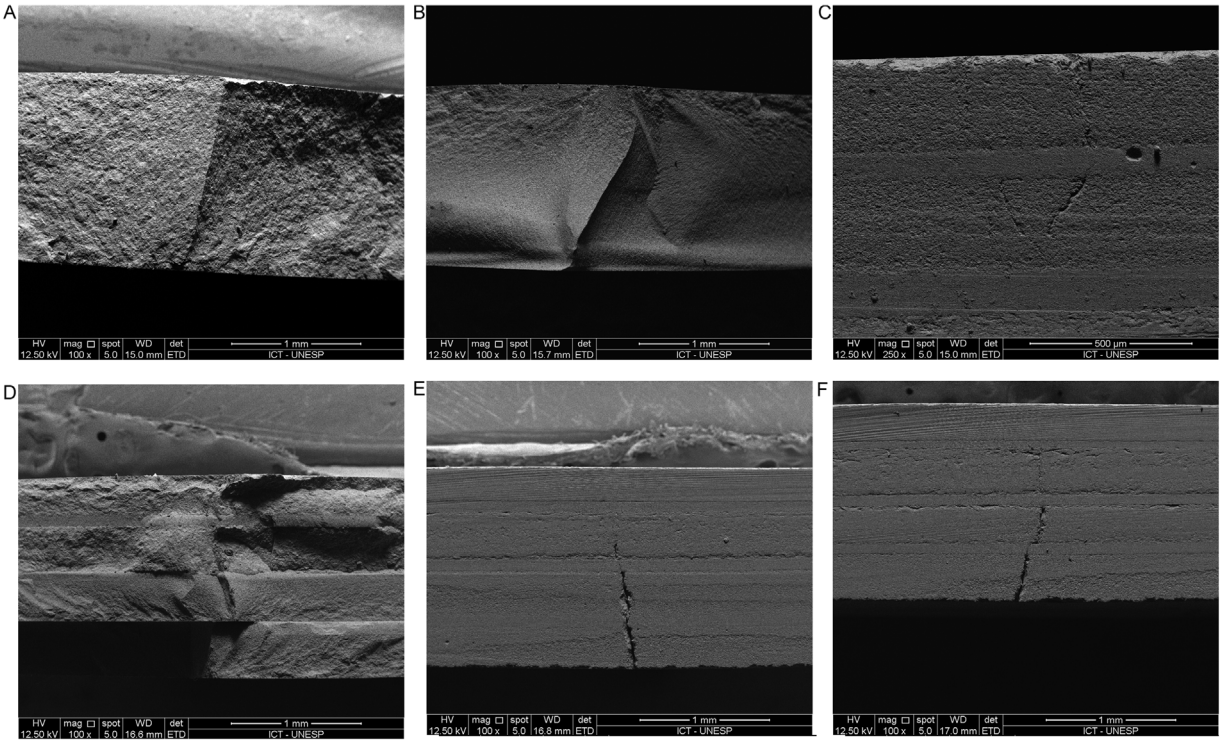

Fig. 4 – Representative micrographs of fractured surfaces (fractographic examination) of all groups after biaxial flexure strength test: ((A) F; (B) L; (C) LLFF; (D) FFLL; (E) YLFF; (F) YLLF). The red arrows indicate the fracture origins initiated in the tension region. The yellow arrows indicate the crack propagation direction into the ceramic layers and the white arrows indicate the hackle lines. (For interpretation of the references to colour in this figure legend, the reader is referred to the web version of this article.)

The monotonic test was conducted to determine the load-to-fracture of the specimens, as recognized by the American Society for Testing and Materials for strength testing of ceramic substrates and by international standard for evaluating dental ceramics [28]. The groups in which the feldspathic ceramic was under tensile stress presented the lowest fracture load values in both monotonic and biaxial flexural fatigue tests (Fig. 1, Table 2). This finding is probably related to the fact that the origin of the fracture and the fracture load of the multilayer configuration are dependent on the material that is directly subjected to the tensile stress [29–31]. Furthermore, the maximum tensile stress in the biaxial flexural configuration is located in the central area of the bottom surface of the disc, between the supporting spheres [28]. Therefore, a similar mechanical behavior was encountered for monolithic and multilayered structures.

The flexural fatigue test was performed for preventing an overestimation of the load-to-fracture of the ceramic structures [32], and predict the failure when applying intermittent cyclical loading. Fatigue is a failure mode that occurs due to progressive brittle cracking under repeated cyclical stresses with intensity below the material strength [33]. As expected for all groups, there was a significant reduction in the fracture load values of at least 40% (Table 2) from the monotonic to fatigue findings due to a sub-critical slow crack growth (SCG) process. The SCG process in dental ceramics is accelerated in the presence of an aqueous environment because of the corrosion process triggered in the interaction of water molecules with the ceramic microcracks and grain boundaries. As the current tests were run under water, the SCG process was accelerated [10].

From the monotonic biaxial test, it was noted that the multilayer structures of YLLF and FFLL had better performance than the feldspathic monolithic group, but they obtained worse results when compared to the monolithic L group. However, the YLLF group did not perform at the same way in the fatigue test, and presented 59% of reduction in fracture load, which was lower than the other groups. A recent study demonstrated that the feldspathic ceramic is less susceptible to SCG than lithium disilicate ceramic [34], which could be related to this behavior. Then, the first zirconia layer in the YLLF group contributed to strengthening, but the lithium disilicate layers contributed to weaken the structure, added to the fact that the thickness of 0.3 mm is too thin in this study configuration. This weakening of the YLLF group also evidences the role of the adhesive interface.

The use of a cement layer was based on the fact that adhesive bonds offer a simple means of joining ceramic brittle layers and this method did not introduce the residual stress intrinsic from the sintering process with the conventionally sintered veneer-ceramic systems due to the differences in coefficient of thermal expansion [35]. Moreover, strong bonding prevents transversal cracks and delamination within the ceramic layers [36], as observed in the multilayered groups. However, the adhesive bond involves different materials and demands additional steps that may result in incorporating

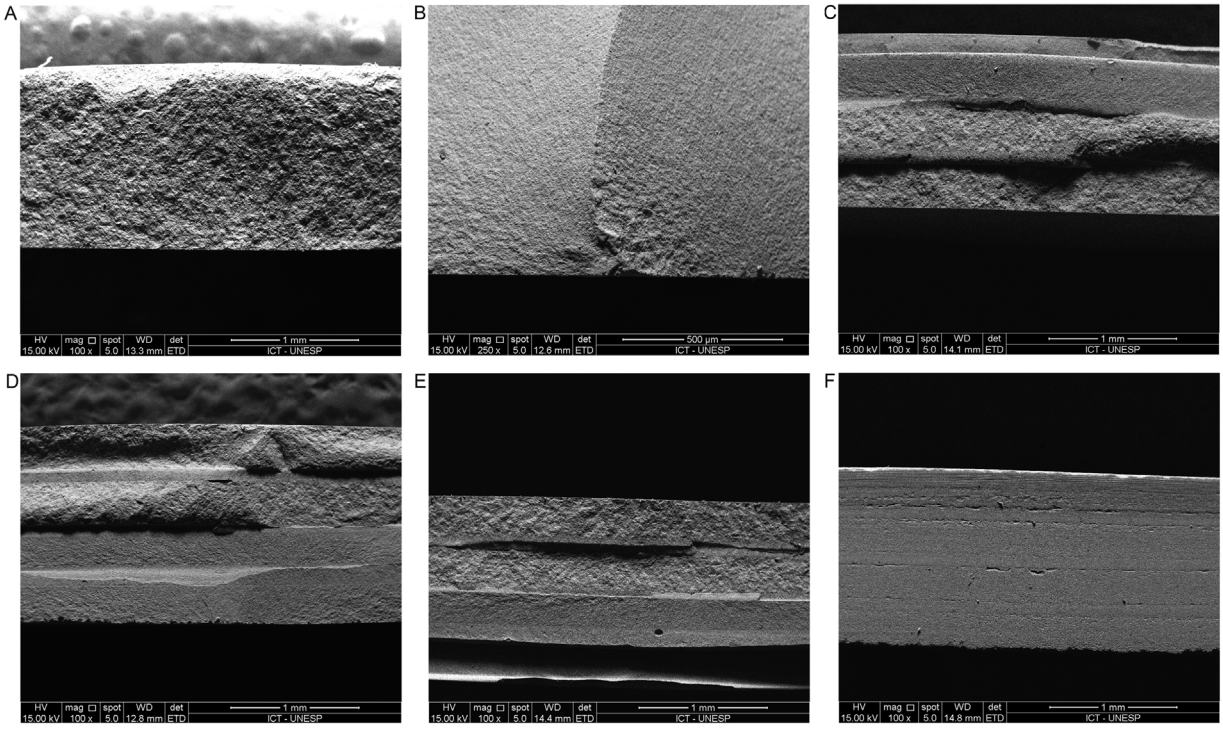

Fig. 5 – Representative micrographs of fractured surfaces (fractographic examination) of all groups after fatigue test: ((A) F; (B) L; (C) LLFF; (D) FFLL; (E) YLFF; (F) YLLF). The red arrows indicate the fracture origins initiated in the tension region. The yellow arrows indicate the crack propagation direction into the ceramic layers. The white arrows indicate the hackle lines and the dashed lines indicate the Wallner's lines arc. (For interpretation of the references to colour in this figure legend, the reader is referred to the web version of this article.)

flaws, and in this case a different ceramic composition was presented in each layer. This forms hybrid layers and interdiffusion zones with their own properties, which may result in a significant reduction of the fatigue strength as observed in our results [32]. Another fact that must be considered is that the YLLF group was the only configuration where the three lowest layers in the region subjected to the tensile stress were composed of three different elastic moduli (feldspathic–cement–lithium disilicate), which could explain the different performance in the mechanical tests.

The graded structures with highest E modulus in the top surface did not fail catastrophically, in contrast to what was observed in the monolithic groups. The inferior layers failed, but the crack did not reach the top ceramic layer, demonstrating that the highest E modulus in the top layer is effective in blocking the crack. Furthermore, the MPS generated in the Y layer in bioinspired configurations is below the MPS in the lowest F layer. Therefore, it is reasonable to expect that the multilayer arrangement may be improved to achieve better results.

Multilayer structures showed similar fracture patterns and fracture origin to monolithic structures. As observed in the top view of the specimens (Fig. 4), the radial crack pattern is the fracture mode for all the specimens, as encountered in multilayer dental structures with glass top layers [12,37]. The crack originated from the ceramic surface at the tensile region for all the specimens; in the graded specimens, the crack crosses through the cement layer and propagates throughout the ceramic layers, which could be explained due to differences in elastic modulus and fracture strength between the cement and ceramic layers. No delamination was observed because the stress to promote fracture did not exceed the interface fracture energy [38]. Nevertheless and contrary to previous studies, the use of an adhesive interface in the multilayer discs did not change the fracture pattern and did not produce an effective strength improvement in the layered configurations [24].

The FEA corroborates these findings and presents the highest maximum principal stress value (MPS) in the tensile region of the models [39]. However, the zirconia layer in the bioinspired configurations presented higher MPS than the inferior layers, except in the most inferior feldspathic layer. These zirconia layers correspond to SEM images where it is noted that the crack did not cross through these layers, since the zirconia material presents a higher flexural strength than the MPS generated during the finite element analysis and in the load-to-fracture in the biaxial flexural strength test.

The predetermined cement thickness of 100 μm was idealized considering that the thinner the cement layer, the higher the strength of the ceramic restorations [40]. In multilayer models, the use of a 30 μm cement layer produced the highest MPS values, while the use of a 100 μm cement layer presented lower values of MPS [41]. Ceramic thickness is another parameter to be considered, since a final thickness of 1.5 mm was

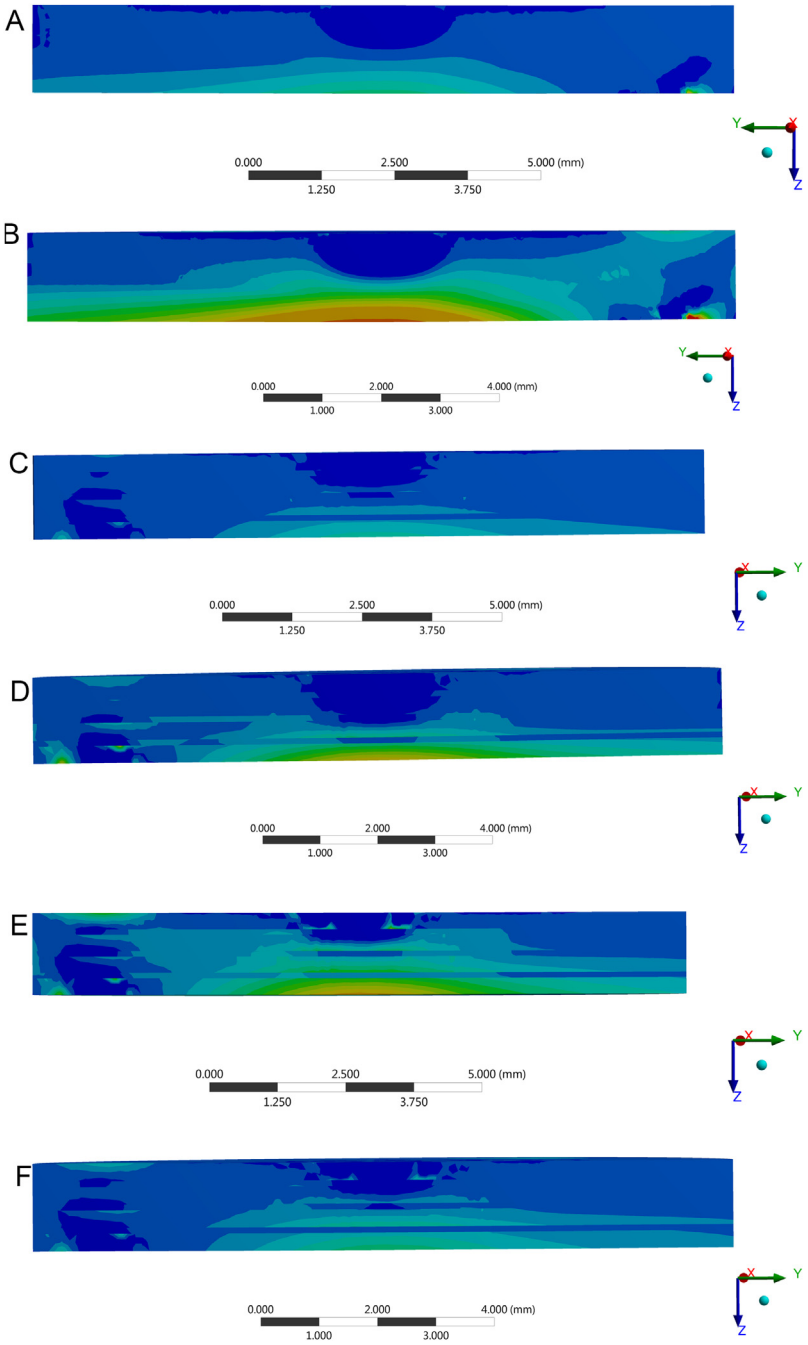

Fig. 6 – Maximum principal stress (MPS) distributions in the dental multilayer structures. Note that in monolithic groups the values were pointed at the corresponding region of the layers used at multilayer samples. Applied load: (A) 177 N; (B) 650 N; (C)147 N; (D) 330 N; (E)150 N; (F) 235 N. The MPS generated in each ceramic in the layers was below the predicted flexural strength of the materials [27].

predetermined in the present study as being recommended for ceramic restorations [42]. This is in accordance with a previous study in which 2 mm ceramic layers presented higher MPS values when compared to 1 mm and 1.5 mm ceramic layers [41]. Moreover, thinner configurations of graded restorations analyzed by FEA of 200 μm produced higher MPS than 1200 μm thickness, revealing an ideal thickness of 1.5 mm [20]. In addition, the lower the veneering ceramic thickness, the higher the flexural strength of the ceramic restoration [43]; moreover, optical properties are highly correlated and can be affected by the thickness of both core and veneer ceramics [44]. Despite these considerations, other studies [45,46] pointed that the thickness of the core veneer has minimal influence on the strength of bilayered systems subject to cyclic loading if the total thickness of ceramic is maintained. Therefore the ceramic material subjected to tensile stresses is mandatory to determine the fatigue behavior of the materials and, the individual thickness layer of 0.3 mm was the weakest because the

adhesive interface was not strong and stiff enough to produce a homogeneous structure acting as a monoblock.

The load-to-fracture of the configurations presented in this study may be related to the maximum bite force (MBF) pointed out in previous studies. The MBF measurement is defined as a parameter indicating the functional condition of the masticatory system [47]. In healthy individuals with normal occlusion, this MBF varies from 93 N to 150 N in the anterior region [48], 424 N to 583 N in the premolar [49] and 424 N to 630 N in the molar region [47]. Considering that the percentage of the MBF varies from 7.7% to 36.2% in natural movements of the mouth such as clenching, opening, and at occlusion [50], it is reasonable to attest that the concept of graded multilayer restorations still needs to be improved, since a restoration made from this concept could be used in anterior region, but it should be avoided in the posterior region of the arc due to the risk of fracture and premature failure.

In this sense, a possible alternative could be the use of an interlayer with similar elastic modulus and coefficient of thermal expansion of the ceramic materials. This could be achieved with a fusion glass layer commonly used in the CAD-on technique which presents an elastic modulus of 65 GPa [51,52], nearest to the feldspathic ceramic blocks which present the value of 64 GPa and a coefficient of thermal expansion of about $9.5 \times 10^{-6}\,K^{-1}$, similar to those of ceramic materials. In addition, this technique could prevent the flawed incorporation inherent to the adhesion procedure and favors the fracture behavior, similar to what occurs in monolithic zirconia restorations [52]. The interlayer would be sufficiently stiff to avoid the flexure of the outer ceramic layer, which decreases the incidence of failures as a result of the multilayer behavior as a homogeneous structure [31,36].

The method presented in this paper for stress distribution between ceramic materials arranged in layers was focused on the elastic properties of the materials in order to build a graded structure. Nonetheless, it was noted that each type of ceramic material and their limitations related to composition, thickness, strength, adhesion properties and aesthetic characteristics must be considered. Furthermore, the disc-shaped simplified model cannot reproduce or represent the mechanical behavior of the ceramic crown complex geometry. Thus, the efforts must be focused on improving the graded concept in order to obtain beneficial effects with this material structure.

5. Conclusion

Within the limits of this study, it was possible to conclude that:

- The material under tensile stress is determinant for the strength of the restoration.
- The adhesive interface negatively influenced the mechanical behavior of the multilayer structures.
- Further investigation considering a homogeneous structure should be performed to evaluate the concept of a restoration with different elastic modulus from the outermost to the innermost layer.

REFERENCES

[1] Kelly JR, Nishimura I, Campbell SD. Ceramics in dentistry: historical roots and current perspectives. J Prosthet Dent 1996;75:18–32.
[2] Wang X, Fan D, Swain MV, Zhao K. A systematic review of all-ceramic crowns: clinical fracture rates in relation to restored tooth type. Int J Prosthodont 2012;25:441–50.
[3] Della Bona A, Kelly JR. The clinical success of all-ceramic restorations. J Am Dent Assoc 2008;139:8S–13S.
[4] Zimmer S, Göhlich O, Rüttermann S, Lang H, Raab WH, Barthel CR. Long-term survival of Cerec restorations: a 10-year study. Oper Dent 2008;33:484–7.
[5] Sailer I, Makarov NA, Thoma DS, Zwahlen M, Pjetursson BE. All-ceramic or metal-ceramic tooth-supported fixed dental prostheses (FDPs)? A systematic review of the survival and complication rates. Part I: single crowns (SCs). Dent Mater 2015;3:603–23.
[6] Ioannidis A, Bindl A. Clinical prospective evaluation of zirconia-based three-unit posterior fixed dental prostheses: up to ten year results. J Dent 2016;47:80–5.
[7] Jian T, Tang MV, Swain X, Wang KZ. Effect of core ceramic grinding on fracture behavior of bilayered zirconia veneering ceramic systems under two loading schemes. Dent Mater 2016;32:1453–63.
[8] Pjetursson BE, Sailer I, Makarov NA, Zwahlen M, Thoma DS. All-ceramic or metal-ceramic tooth-supported fixed dental prostheses (FDPs)? A systematic review of the survival and complication rates. Part II: multiple-unit FDPs. Dent Mater 2015;31:624–39.
[9] Rizkalla AS, Jones DW. Mechanical properties of commercial high strength ceramic core materials. Dent Mater 2004;20:207–12.
[10] Morena R, Lockwood PE, Fairhurst CW. Fracture toughness of commercial dental porcelains. Dent Mater 1986;2:58–62.
[11] Huang M, Rahbar N, Wang R, Thompson V, Rekow D, Soboyejo WO. Bioinspired design of dental multilayers. J Mater Sci Eng A 2007;464:315–20.
[12] Niu X, Yang Y, Soboyejo W. Contact deformation and cracking of zirconia/cement/foundation dental multilayers. J Mater Sci Eng A 2008;485:517–23.
[13] Niu X, Rahbar N, Farias S, Soboyejo W. Bio-inspired design of dental multilayers: experiments and model. J Mech Behav Biomed Mater 2009;2:596–602.
[14] Du J, Niu X, Soboyejo W. Creep-assisted slow crack growth in bio-inspired dental multilayers. J Mech Behav Biomed Mater 2015;46:41–8.
[15] Bajaj D, Arola D. Role of prism decussation on fatigue crack growth and fracture of human enamel. Acta Biomater 2009;5:3045–56.
[16] Zhang YR, Du W, Zhou XD, Yu HY. Review of research on the mechanical properties of the human tooth. Int J Oral Sci 2014;6:61–9.
[17] Madfa AA, Yue X-G. Dental prostheses mimic the natural enamel behavior under functional loading: a review article. Jpn Dent Sci Rev 2016;52:2–13.
[18] Deng Y, Miranda P, Pajares A, Guiberteau F, Lawn BR. Fracture of ceramic/ceramic/polymer trilayers for biomechanical applications. J Biomed Mater Res A 2003;67(3):828–33.
[19] Lawn BR, Deng Y, Lloyd IK, Janal MN, Rekow ED, Thompson VP. Materials design of ceramic-based layer structures for crowns. J Dent Res 2002;81(6):433–8.
[20] Rahbar N, Soboyejo WO. Design of functionally graded dental multilayers. Fatigue Fract Engng Mater Struct 2011;34:887–97.
[21] Lin CP, Douglas WH, Erlandsen SL. Scanning electron microscopy of type I collagen at the dentin-enamel junction

of human teeth. J Histochem Cytochem 1993;41:381–8.
[22] Borba M, Araújo MD, Lima E, Yoshimura HN, Cesar PF, Griggs JA, et al. Flexural strength and failure modes of layered ceramic structures. Dent Mater 2011;27:1259–66.
[23] Belli R, Wendler M, de Ligny D, Cicconi MR, Petschelt A, Peterlik H, et al. Chairside CAD/CAM materials. Part 1: measurement of elastic constants and microstructural characterization. Dent Mater 2017;33(1):84–98.
[24] Costa AK, Borges AL, Fleming GJ, Addison O. The strength of sintered and adhesively bonded zirconia/veneer-ceramic bilayers. J Dent 2014;42(10):1269–76.
[25] Schmitter M, Schweiger M, Mueller D, Rues S. Effect on in vitro fracture resistance of the technique used to attach lithium disilicate ceramic veneer to zirconia frameworks. Dent Mater 2014;30(2):122–30.
[26] Collins JA. Failure of materials in mechanical design: analysis, prediction, prevention. 2nd ed. New York: John Wiley Sons; 1993.
[27] Zhang Y, Kelly JR. Dental ceramics for restoration and metal veneering. Dent Clin North Am 2017;61:797–819.
[28] Huang CW, Hsueh CH. Piston-on-three-ball versus piston-on-ring in evaluating the biaxial strength of dental ceramics. Dent Mater 2011;27:e117–23.
[29] Della Bona A, Anusavice KJ, DeHoff PH. Weibull analysis and flexural strength of hot-pressed core and veneered ceramic structures. Dent Mater 2003;19:662–9.
[30] Guazzato M, Albakry M, Ringer SP, Swain MV. Strength, fracture toughness and microstructure of a selection of all-ceramic materials. Part II. Zirconia-based dental ceramics. Dent Mater 2004;20:449–56.
[31] Basso GR, Moraes RR, Borba M, Griggs JA, Della Bona A. Flexural strength and reliability of monolithic and trilayer ceramic structures obtained by the CAD-on technique. Dent Mater 2015;31:1453–9.
[32] Arola D. Fatigue testing of biomaterials and their interfaces. Dent Mater 2017;33:367–81.
[33] Wiskott HW, Nicholls JI, Belser UC. Stress fatigue: basic principles and prosthodontic implications. Int J Prosthodont 1995;8:105–16.
[34] Ramos NC, Campos TM, Paz IS, Machado JP, Bottino MA, Cesar PF, et al. Microstructure characterization and SCG of newly engineered dental ceramics. Dent Mater 2016;32(7):870–8.
[35] Benetti P, Kelly JR, Sanchez M, Della Bona A. Influence of thermal gradients on stress state of veneered restorations. Dent Mater 2014;30:554–63.
[36] Lee JJW, Lloyd IK, Chai H, Jung YG, Lawn BR. Arrest, deflection, penetration and reinitiation of cracks in brittle layers across adhesive interlayers. Acta Mater 2007;55(17):5859–66.
[37] Niu X, Soboyejo WO. Effects of loading rate on the deformation and cracking of dental multilayers: experiments and models. J Mater Res 2006;21:970–5.
[38] Thompson GA. Influence of relative layer height and testing method on the failure mode and origin in a bilayered dental ceramic composite. Dent Mater 2000;16:235–43.
[39] Guazzato M, Proos K, Quach L, Swain MV. Strength, reliability and mode of fracture of bilayered porcelain/zirconia (Y-TZP) dental ceramics. Biomaterials 2004;25:5045–52.
[40] May LG, Kelly JR, Bottino MA, Hill T. Influence of the resin cement thickness on the fatigue failure loads of CAD/CAM feldspathic crowns. Dent Mater 2015;31:895–900.
[41] Kurtoglu C, Uysal H, Mamedov A. Influence of layer thickness on stress distribution in ceramic-cement-dentin multilayer systems. Dent Mater J 2008;27:626–32.
[42] Volpato CA, Monteiro Jr S, de Andrada MC, Fredel MC, Petter CO. Optical influence of the type of illuminant, substrates and thickness of ceramic materials. Dent Mater 2009;25:87–93.
[43] Benetti P, Pelogia F, Valandro LF, Bottino MA, Bona AD. The effect of porcelain thickness and surface liner application on the fracture behavior of a ceramic system. Dent Mater 2011;27:948–53.
[44] Wang F, Takahashi H, Iwasaki N. Translucency of dental ceramics with different thicknesses. J Prosthet Dent 2013;110:14–20.
[45] Dibner AC, Kelly JR. Fatigue strength of bilayered ceramics under cyclic loading as a function of core veneer thickness ratios. J Prosthet Dent 2016;115(March (3)):335–40.
[46] Hsueh C-H, Miranda P. Modeling of contact-induced radial cracking in ceramic bilayer coatings on compliant substrates. J Mater Res 2003;18:1275–83.
[47] Abreu RA, Pereira MD, Furtado F, Prado GP, Mestriner Jr W, Ferreira LM. Masticatory efficiency and bite force in individuals with normal occlusion. Arch Oral Biol 2014;59:1065–74.
[48] Paphangkorakit J, Osborn JW. The effect of pressure on a maximum incisal bite force in man. Arch Oral Biol 1997;42(1):11–7.
[49] Van Eijden TM. Three-dimensional analyses of human bite-force magnitude and moment. Arch Oral Biol 1991;36(7):535–9.
[50] Gibbs CH, Mahan PE, Lundeen HC, Brehnan K, Walsh EK, Holbrook WB. Occlusal forces during chewing and swallowing as measured by sound transmission. J Prosthet Dent 1981;46:443–9.
[51] Kanat B, Cömlekoğlu EM, Dündar-Çömlekoğlu M, Hakan Sen B, Ozcan M, Ali Güngör M. Effect of various veneering techniques on mechanical strength of computer-controlled zirconia framework designs. J Prosthodont 2014;23:445–55.
[52] Alessandretti R, Borba M, Benetti P, Corazza PH, Ribeiro R, Della Bona A. Reliability and mode of failure of bonded monolithic and multilayer ceramics. Dent Mater 2017;33:191–7.